Sports Medicine (2023) 53:1651–1665
https://doi.org/10.1007/s40279-023-01846-9

ORIGINAL RESEARCH ARTICLE

Metabolic Signatures of Performance in Elite World Tour Professional Male Cyclists

Travis Nemkov[1] · Francesca Cendali[1] · Davide Stefanoni[1] · Janel L. Martinez[2] · Kirk C. Hansen[1] · Iñigo San-Millán[2,3] · Angelo D'Alessandro[1,4]

Accepted: 19 March 2023 / Published online: 6 May 2023

Abstract

Background and Objective Metabolomics studies of recreational and elite athletes have been so far limited to venipuncture-dependent blood sample collection in the setting of controlled training and medical facilities. However, limited to no information is currently available to determine if findings in laboratory settings are translatable to a real-world scenario in elite competitions. The goal of this study was to define molecular signatures of exertion under controlled exercise conditions and use these signatures as a framework for assessing cycling performance in a World Tour competition.

Methods To characterize molecular profiles of exertion in elite athletes during cycling, we performed metabolomics analyses on blood isolated from 28 international-level, elite, World Tour professional male athletes from a Union Cycliste Internationale World Team taken before and after a graded exercise test to volitional exhaustion and before and after a long aerobic training session. Moreover, established signatures were then used to characterize the metabolic physiology of five of these cyclists who were selected to represent the same Union Cycliste Internationale World Team during a seven-stage elite World Tour race.

Results Using dried blood spot collection to circumvent logistical hurdles associated with field sampling, these studies defined metabolite signatures and fold change ranges of anaerobic or aerobic exertion in elite cyclists, respectively. Blood profiles of lactate, carboxylic acids, fatty acids, and acylcarnitines differed between exercise modes. The graded exercise test elicited significant two- to three-fold accumulations in lactate and succinate, in addition to significant elevations in free fatty acids and acylcarnitines. Conversely, the long aerobic training session elicited a larger magnitude of increase in fatty acids and acylcarnitines without appreciable increases in lactate or succinate. Comparable signatures were revealed after sprinting and climbing stages, respectively, in a World Tour race. In addition, signatures of elevated fatty acid oxidation capacity correlated with competitive performance.

Conclusions Collectively, these studies provide a unique view of alterations in the blood metabolome of elite athletes during competition and at the peak of their performance capabilities. Furthermore, they demonstrate the utility of dried blood sampling for omics analysis, thereby enabling molecular monitoring of athletic performance in the field during training and competition.

✉ Travis Nemkov
travis.nemkov@cuanschutz.edu

✉ Angelo D'Alessandro
angelo.dalessandro@cuanschutz.edu

[1] Department of Biochemistry and Molecular Genetics, Anschutz Medical Campus, University of Colorado, 12801 East 17th Ave L18-9122, Aurora, CO 80045, USA

[2] Department of Medicine, Division of Endocrinology, Metabolism and Diabetes, University of Colorado, Anschutz Medical Campus, Aurora, CO, USA

[3] Department of Human Physiology and Nutrition, University of Colorado, Colorado Springs, CO, USA

[4] Department of Biochemistry and Molecular Genetics, University of Colorado, Anschutz Medical Campus, 12801 East 17Th Ave L18-9118, Aurora, CO 80045, USA

Key Points

We profiled the metabolism of 28 international-level, elite, World Tour professional male athletes from a Union Cycliste Internationale World Team during training and a World Tour multi-stage race.

Dried blood spot sampling affords metabolomics analyses to monitor exercise performance.

Determination of lactate thresholds during a graded exercise test to volitional exhaustion shows a range of 3.75–6.5 W/kg in this group.

Blood profiles of lactate, carboxylic acids, fatty acids, and acylcarnitines differed between different exercise modes (graded exercise test and 180-km aerobic training session).

Metabolic profiles were affected by stage-specific challenges (sprint vs climbing) during a World Tour multi-stage race.

1 Introduction

Investigations into the metabolic effects of exercise [1, 2] have helped elucidate physiological adaptations to stress and have been critical for understanding pathologies in which metabolism is dysregulated. From aging [3] to cardiovascular and other non-communicable diseases [4, 5], from cancer [6] to hemorrhagic or ischemic hypoxia [7], from immunometabolism [8] to neurodegenerative diseases [9], metabolic derangements are increasingly appreciated as etiological contributors to disease onset, severity, and prognosis.

Energy requirements and substrate utilization during physical exertion are dependent upon workload and the perfusion of oxygen. During low- and medium-intensity exercise when oxygen supply is sufficient to meet bioenergetic demands, fatty acid substrates are relied upon for the generation of adenosine triphosphate (ATP) through the use of fatty acid oxidation to fuel the tricarboxylic acid (TCA) cycle. As exertional intensity increases to a point where oxidative phosphorylation is no longer sufficient, metabolism shifts to favor the rapidity of carbohydrate-driven glycolysis for ATP generation, a metabolic switch that increases the rate of lactate formation. Under high glycolytic rates, lactate production exceeds the rate of lactate consumption in the mitochondria and thus begins to accumulate in circulation [10]. While lactate is primarily formed in fast-twitch fibers, it is oxidized during exercise as a substrate to fuel mitochondria of adjacent slow-twitch muscle fibers. A metabolic inflection point, called the "lactate threshold" (LT), is defined by the maximal effort or intensity that an athlete can maintain for an extended period of time with little or no increase in circulating lactate [11]. As such, classic studies have focused on LT as a proxy for exercise performance.

In the last decade, there has been an increased focus on the metabolic responses to exercise including measurement of substrate utilization, metabolic flexibility, and mitochondrial function in athletes [12]. Recent advances in metabolomics have fostered a more comprehensive understanding of human responses to low-, moderate-, or high-intensity exercise [13, 14]. Results have evidenced a differential impact of exercise modes (e.g., acute vs resistance and endurance exercise [15]) and across different sports (e.g., endurance athletes, sprinters, bodybuilders [16, 17]) on the extent and magnitude of metabolic reprogramming. While we have recently reported metabolomics-based characterizations of cycling in recreational [18] and professional [19] athletes under controlled acute training regimens, the literature is scarce on elite professional athletes undergoing testing in the field and, more importantly, during World Tour competitions. As such, we hypothesized that analyzing blood metabolite signatures before and after controlled training sessions with varying degrees of exertion could provide insights into exertion during competition and correlate with competitive performance. Performing such investigations in elite professional athletes offers a unique opportunity to determine the ceiling of human performance, against which we can scale human physiology of healthy occasional, recreational, semi-professional, and professional athletes. Such a scale would also inform a model on how human metabolism works at its optimum, which in turn could drive the interpretation of metabolic derangements under pathological conditions, even at their early onset.

2 Methods

2.1 Subjects

Twenty-eight members of an elite male cycling team competing at the Union Cycliste Internationale World Tour level were recruited for these studies. Identifying details of these cyclists were intentionally omitted to maintain anonymity. Anthropometric characteristics of these subjects are provided in Table 1 of the Electronic Supplementary Material (ESM). The inclusion criteria required that each cyclist was approved for training or competition by a team doctor. In preparation for testing, all cyclists reported to the laboratory in a fasted state of at least 1 h and abstained from alcohol and caffeine for at least 8 h prior to testing. Additionally, none of the cyclists were on a carbohydrate-restricted diet and they consumed their normal diet. To minimize the impact of recent physical activity on the results, all cyclists abstained from strenuous physical activity for 24 h prior to testing.

2.2 Graded Exercise Test

Twenty-eight cyclists from the recruited cohort performed a graded exercise test (GXT) to exhaustion on an electrically controlled, resistance leg cycle ergometer (Elite, Suito, Italy). After a 15 min warm-up (exercise intensity < 100 W), participants started leg cycling at a low intensity of 1.5 $W \cdot kg^{-1}$ of body weight. Cycling intensity was increased 0.5 $W \cdot kg^{-1}$ every 10 min as previously described [12]. Power output and heart rate were monitored continuously throughout the test (Wahoo Fitness, Atlanta, GA, USA). Blood lactate levels were measured at the end of every intensity stage through capillary extraction (Lactate Plus; Nova Medical, Houston, TX, USA) as described [12].

2.3 Aerobic Training Session

Two days after the GXT, 27 of the 28 cyclists then completed a 180 km training ride over 5:20 h (the remaining cyclist from the GXT was unable to train this day). Cyclists were required to maintain a power output between 3.0 and 3.5 $W \cdot kg^{-1}$ on flat terrain. During the ride, each cyclist was required to perform three 10.6-km climbs with an average inclination grade of 6.8% at their individual LT (as determined by the GXT). Each climb was separated by a 45-min interval maintained at 3.0–3.5 $W \cdot kg^{-1}$ except for the climb descent, which was approximately 10 min. The final 40 km of the training ride were performed at low aerobic intensity (< 3.0 $W \cdot kg^{-1}$).

2.4 Blood Sampling for Metabolomics

Twenty microliters of whole blood was sampled before and after the GXT and the aerobic training session using a Mitra® Volumetric Absorptive Sampling (VAMS) device and dried under ambient conditions according to manufacturer's instructions (Neoteryx, Torrance, CA, USA). Samples were individually sealed in air-tight packaging in the presence of a desiccant and shipped under ambient conditions to the University of Colorado Anschutz Medical Campus. Upon arrival, individual samples were added to 200 µL of methanol:acetonitrile:water (5:3:2 v/v/v) and sonicated for 1 h as described [20, 21]. Metabolite extracts were isolated by centrifugation at 18,000×*g* for 10 min. Supernatants were separated into autosampler vials.

2.5 World Tour Stage Race

Five of the 28 cyclists profiled in the GXT and aerobic training test were selected to represent a Union Cycliste Internationale World Team by the team's coaching staff and participated in a seven-stage elite World Tour race. The date and location of the race are intentionally omitted to preserve anonymity of the subjects. Performance parameters such as speed and power output were monitored using Training Peaks (Louisville, CO, USA). Because of logistical constraints, whole blood samples were collected using the TAP device (Seventh Sense Biosystems, Medford, MA, USA) as previously described [22] prior to and immediately upon completion of Stages 1, 4, and 6. Samples were frozen in dry ice within 15 min of isolation and were maintained under this condition until all samples were collected, upon which they were shipped on dry ice to the analytical laboratory and stored at − 80 °C until analysis.

2.6 Sample Preparation

Prior to ultra-high performance liquid chromatography-mass spectrometry analysis, samples were placed on ice and re-suspended with 9 volumes of ice cold methanol:acetonitrile:water (5:3:2, v:v) and vortexed continuously for 30 min at 4 °C for metabolomics or 9 volumes of ice cold methanol and incubated for 30 min at − 20 °C for lipidomics. Prior to sample resuspension, the metabolomics extraction solution was supplemented with final concentrations of 0.5 µM of $^{13}C^{15}N$ amino acid mixture, 40 µM of $^{13}C_1$-lactate, and 50 µM of $^{13}C_6$-glucose (Cambridge Isotope Laboratories, Inc., Tewksbury, MA, USA) for determination of the absolute molar concentration of analytes. Insoluble material was removed by centrifugation at 18,000*g* for 10 min at 4 °C and supernatants were isolated for omics analysis by ultra-high performance liquid chromatography-mass spectrometry. Metabolite extracts were dried down under a speed vacuum and re-suspended in an equal volume of 0.1% formic acid prior to analysis, while lipidomics extracts were analyzed in methanol.

2.7 Ultra-High Performance Liquid Chromatography-Mass Spectrometry Data Acquisition and Processing

Analyses were performed as previously published [23, 24]. Briefly, the analytical platform employs a Vanquish ultra-high performance liquid chromatography system (Thermo Fisher Scientific, San Jose, CA, USA) coupled online to a Q Exactive mass spectrometer (Thermo Fisher Scientific). Polar extracts (2-µL injections) were resolved over a Kinetex C18 column, 2.1 × 150 mm, 1.7-µm particle size (Phenomenex, Torrance, CA, USA) equipped with a guard column (SecurityGuard™ Ultracartridge, UHPLC C18 for 2.1-mm ID Columns, AJO-8782; Phenomenex) using an aqueous phase (A) of water and 0.1% formic acid and a mobile phase (B) of acetonitrile and 0.1% formic acid for positive ion polarity mode, and an aqueous phase (A) of water:acetonitrile (95:5) with 1 mM of ammonium acetate and a mobile phase (B) of acetonitrile:water (95:5) with 1 mM of ammonium acetate for negative ion polarity mode. The Q Exactive mass spectrometer (Thermo

Fisher Scientific) was operated independently in positive or negative ion mode, scanning in either a full MS mode (2 µscans) from 60 to 900 *m/z* at 70,000 resolution, with a 4-kV spray voltage, 45 sheath gas, 15 auxiliary gas, AGC target = 3e6, maximum IT = 200 ms or data-dependent fragmentation (Top 15 ddMS2, for validation) at 17,500 resolution, AGC target = 1e5, maximum IT = 200 ms, isolation window = 4.0 *m/z*, NCE = 20, 24, 28. Non-polar lipid extracts were resolved over an ACQUITY HSS T3 column (2.1 × 150 mm, 1.8-µm particle size; Waters, Milford, MA, USA) using an aqueous phase (A) of 25% acetonitrile and 5 mM of ammonium acetate and a mobile phase (B) of 90% isopropanol, 10% acetonitrile, and 5 mM of ammonium acetate. The column was equilibrated at 30% B, and upon injection of 10 µL of extract, samples were eluted from the column using the solvent gradient: 0–9 min 30–100% B at 0.325 mL/min; hold at 100% B for 3 min at 0.3 mL/min, and then decrease to 30% over 0.5 min at 0.4 mL/min, followed by a re-equilibration hold at 30% B for 2.5 min at 0.4 mL/min. The Q Exactive mass spectrometer (Thermo Fisher Scientific) was operated in positive ion mode, scanning in full mass spectrometry mode (2 µscans) from 150 to 1500 *m/z* at 70,000 resolution, with a 4-kV spray voltage, 45 sheath gas, 15 auxiliary gas, AGC target = 3e6, and maximum IT = 200 ms. Data-dependent fragmentation (Top 10 ddMS2) was performed at 17,500 resolution, AGC target = 1e5, maximum IT = 50 ms, and stepped NCE of 25, 35 for positive mode, and 20, 24, and 28 for negative mode. Samples were analyzed in randomized order with a technical mixture injected after every ten samples to qualify instrument performance. Calibration was performed prior to analysis using the Pierce™ Positive and Negative Ion Calibration Solutions (Thermo Fisher Scientific).

2.8 Data Analysis

Acquired data were converted from a raw to mzXML file format using Mass Matrix (Cleveland, OH, USA). Discovery mode alignment, feature identification, and data filtering were performed using Compound Discoverer 3.0 (Thermo Fisher Scientific). Metabolite assignments were performed using accurate intact mass (sub-10 ppm), isotopologue distributions, and retention time/spectral comparison to an in-house standard compound library (MSMLS, IROA Technologies, NJ, USA) using MAVEN (Princeton, NJ, USA) [25]. A coefficient of variation < 20% in the technical mixtures was used as a threshold for reporting metabolites.

Metabolite molar concentrations were determined by multiplying the ratio of the monoisotope to the respective spiked in isotopologue standard by the standard known concentration, with a subsequent correction for the dilution factor during extraction as reported [23]. Lipidomics data were analyzed using LipidSearch 5.0 (Thermo Scientific), which provides lipid identification on the basis of accurate intact mass, isotopic pattern, and fragmentation pattern to determine lipid class and acyl chain composition.

Graphs, heat maps, and statistical analyses (either a *T*-test or analysis of variance), metabolic pathway analysis, partial least squares-discriminant analysis, and hierarchical clustering were performed using the MetaboAnalyst 4.0 package [26]. XY graphs were plotted through GraphPad Prism 8 (GraphPad Software Inc., La Jolla, CA, USA). Pathway graphs were prepared on BioRender.com. Fuzzy c-means clustering was performed using the R package 'Mfuzz' (v2.20.0) using four centers, and an m value of 1.5 and an min.acore of 0.7.

Metabolite pathway enrichment analysis was performed using the Peaks To Pathways of MetaboAnalyst 4.0. Feature regions identified with the longitudinal patterns selected from c-means clustering were subjected to pathway analysis and enrichments were plotted on pie charts demonstrating pathway enrichment as a function of observed versus total pathway hits.

3 Results

3.1 Metabolomic Changes Observed in Blood Vary as a Function of Training Intensity and Duration

In consideration that the LT and the shift between substrate and pathway utilization is dependent upon training status and performance capacity, we sought to identify circulating metabolite profiles of aerobic and anaerobic exertion in the whole blood of elite World Tour professional cyclists during a team training camp using mass spectrometry-based metabolomics. To determine a LT, these cyclists first underwent a GXT to volitional exhaustion, in which progressive increases in power output on an ergometer were accompanied by whole blood lactate measurements (Fig. 1A). A range of LTs from 3.75 to 6.5 $W \cdot kg^{-1}$ was observed in this group, demonstrating variation in metabolic capacity even at the elite level (Fig. 1B). Guided by the LTs determined in the GXT, these cyclists subsequently completed a 180 km aerobic training session within a power output range beneath the LT (Fig. 1B). Importantly, guidance on training power output ranges would not be supported by heart rate monitoring alone, as circulating lactate only moderately correlated with the heart rate over all measured power output ranges ($R^2 = 0.53$, $p < 0.0001$), and this correlation depended on functional output (Fig. 1 of the ESM). As revealed through metabolomics, blood samples taken before and after the GXT could be distinctly grouped based on metabolite signatures using an unsupervised principal component analysis (PCA) (Fig. 1D, Table 1 of the ESM). A partial least squares-discriminant analysis (PLS-DA) model

was developed to identify metabolic characteristics of each timepoint and highlighted glycolysis (pyruvate, lactate), TCA cycle (malate, succinate), nucleotide/nicotinamide metabolism (xanthine, kynurenic acid, ADP-ribose, phosphate), oxidative stress (cystine, γ-glutamyl-alanine), and fatty acid oxidation [β-hydroxybutyrate, AC(2:0), AC(12:0), AC(16:2)] as top contributors to the metabolic character of samples isolated before and after the GXT (Fig. 1E). In comparison, PCA was able to distinguish samples taken before and after the long aerobic training session, with a few samples clustering in the opposite group possibly indicating varying levels of exertion or recovery (Fig. 1F). Timepoints from this training test were predominantly distinguished by acylcarnitines, intermediates of fatty acid oxidation (Fig. 1G).

In addition to the accumulation of lactate during the GXT (intra-individual fold changes of 2.91 ± 0.94), higher levels of glucose (1.35 ± 0.38), phosphoglycerate (1.48 ± 0.59), phospoenolpyruvate (1.27 ± 0.52), and pyruvate (2.34 ± 0.78), in conjunction with lower levels of hexose phosphate (0.81 ± 0.50), indicate ongoing glycogenolysis and committal to glycolysis during this exercise test (Fig. 1H). The accumulation of succinate (2.85 ± 1.06) during the GXT was comparable to lactate, while additional carboxylic acids citrate (1.38 ± 0.61), fumarate (1.36 ± 0.34), and malate (1.66 ± 0.54) were also increased (Fig. 1H). These metabolic profiles were distinct from those observed in the 180-km aerobic training session, where only glucose (1.17 ± 0.32) and succinate (1.28 ± 0.37) were significantly higher after the test, though to a lower extent (Fig. 1I).

Blood profiles of fatty acids and acylcarnitines differed between these two exercise modes as well. While long-chain fatty acids accumulated during both exercise modes, the extent of accumulation was higher after the 180 km aerobic training session and indicated more fatty acid mobilization for energy generation (Fig. 1J, K). Increased levels of short-chain fatty acids and medium-chain fatty acids after the GXT, however, suggest incomplete fatty acid oxidation during this cycling test to volitional exhaustion. In support, post-GXT blood had more abundant short-chain acylcarnitines, while blood post-180 km aerobic training had no changes to short-chain acylcarnitines (SCAC) and higher levels of medium-chain acylcarnitines (MCAC) (Fig. 1L, M). These findings support more reliance on fatty acid oxidation during the entirety of the long aerobic training session, as further exemplified by lower levels of circulating carnitine (0.86 ± 0.22) in comparison to the GXT (Fig. 1L, M).

3.2 Metabolomic Changes Vary Based on Overall Progression of the Multi-Stage World Tour Race

We next sought to determine blood metabolic signatures in five members of this Union Cycliste Internationale elite World Tour Team during competition in a multi-stage World Tour race. To determine how these signatures change as a function of exertion both during individual stages and as a progression throughout the entire competition, whole blood samples were collected prior to and immediately upon completion of Stages 1, 4, and 6 that were characterized by a distance/elevation of 143 km/60 m, 214.5 km/3600 m, and 127.5 km/4300 m, respectively. Once collected, samples were analyzed by untargeted metabolomics and lipidomics using high-throughput mass spectrometry (Fig. 2A). Volcano plots indicated that, as the race progressed, fewer metabolites were significantly depleted during the stage (30, 26, and 11 significant features were higher before the beginning of Stages 1, 4, and 6, respectively), while Stage 6—the most difficult stage—elicited the largest increase in circulating metabolites (Fig. 2B). Untargeted profiles were hierarchically clustered to assess relative abundances as a function of stage and time (Fig. 2C). From the untargeted metabolomics data, spectra for 1971 putative metabolites were manually curated to identify 283 named compounds (Table 1 of the ESM). The PLS-DA of this sample set separated timepoints chronologically across the Component 1 axis (which explained 16.2% of the co-variance; Fig. 2D, left). Samples obtained from all but one of the cyclists after Stages 4 and 6 begin to deviate from a linear progression and spread along the Component 2 axis. Top metabolites that influenced this clustering pattern contained primarily amino acids, free fatty acids, and acylcarnitines (Fig. 2D, right). Considering that the clustering pattern mirrored the chronologic progression of stages, we then analyzed individually the pre- and post-timepoints. The PLS-DA separated samples taken before Stages 1, 4, and 6, indicating a progressive change in baseline blood signatures throughout the race (Fig. 2E, left). These changes related primarily to amino acids (glycine, threonine, serine, 3-hydroxyisobutyrate), nitrogen metabolism (*N*-acetylspermidine), fatty acid metabolism [FA(22:5, 20:3)], glycolysis/energy (glyceraldehyde 3-phosphate, nicotinamide), and oxidative stress (methionine S-oxide, hexose phosphate, sedoheptulose 7-phosphate) (Fig. 2E, right). Meanwhile, samples taken after each stage were even more distinguishable as the race progressed. Two cyclists sampled after Stage 4 clustered with the post-Stage 6 group, suggesting that they were accumulating markers of fatigue earlier on in the race (Fig. 2F, left). The relative similarity of these groups depended predominantly on free fatty acids [FA(20:3, 22:4, 6:0, 16:0, 18:0)], amino acids (glycine, asparagine, serine, glutamine), and energy metabolites (guanosine monophosphate (GMP), pyruvate, fumarate) (Fig. 2F, right).

To identify patterns of metabolite changes throughout the race, we performed c-means clustering (Fig. 2G). Cluster 1 contained molecules that increased during each stage, though to a lower extent as the race went on

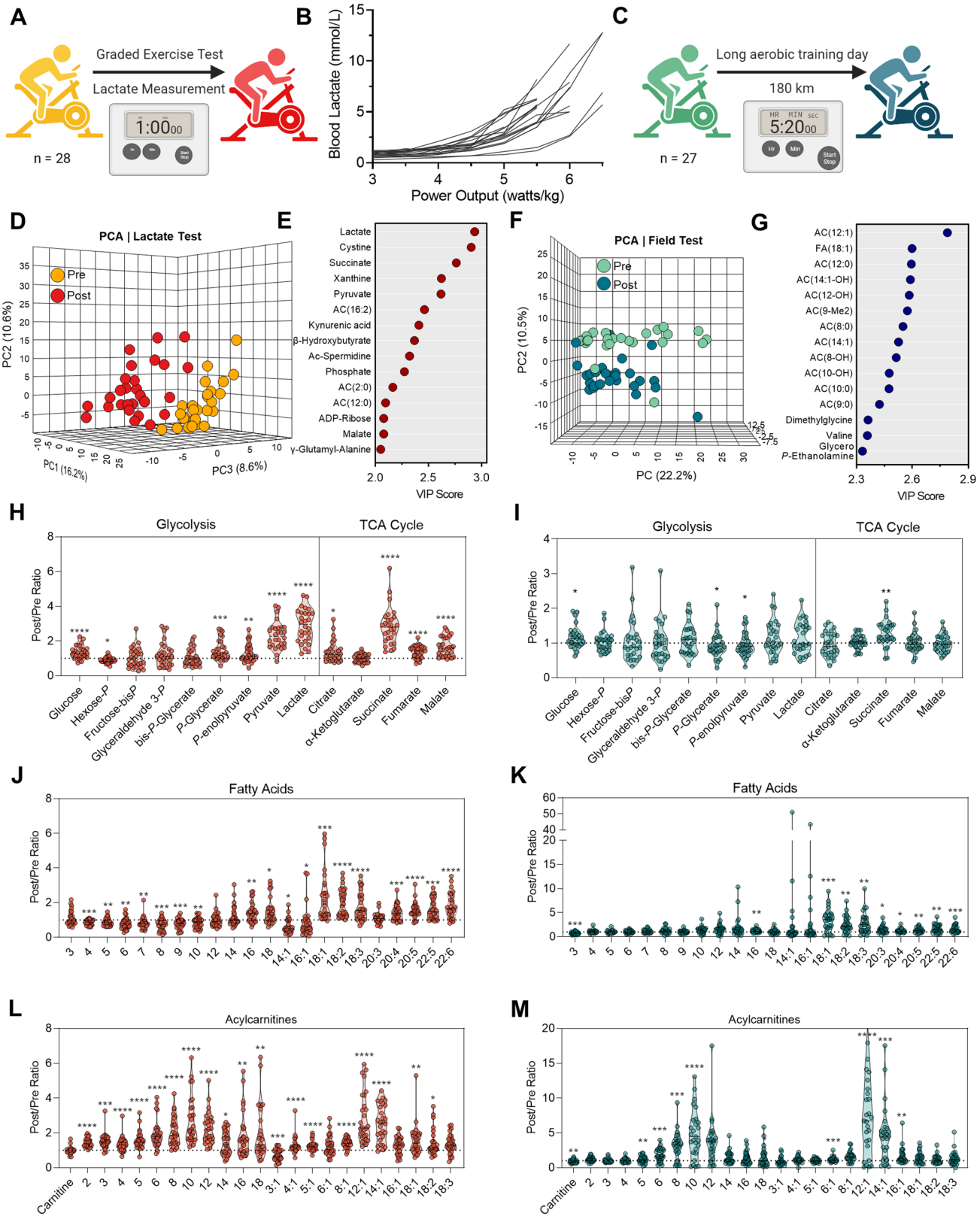
A
Graded Exercise Test
Lactate Measurement
n = 28
B
Blood Lactate (mmol/L)
Power Output (watts/kg)
C
Long aerobic training day
180 km
n = 27
D
PCA | Lactate Test
Pre
Post
PC2 (10.6%)
PC1 (16.2%)
PC3 (8.6%)
E
Lactate
Cystine
Succinate
Xanthine
Pyruvate
AC(16:2)
Kynurenic acid
β-Hydroxybutyrate
Ac-Spermidine
Phosphate
AC(2:0)
AC(12:0)
ADP-Ribose
Malate
γ-Glutamyl-Alanine
VIP Score
F
PCA | Field Test
Pre
Post
PC2 (10.5%)
PC (22.2%)
G
AC(12:1)
FA(18:1)
AC(12:0)
AC(14:1-OH)
AC(12-OH)
AC(9-Me2)
AC(8:0)
AC(14:1)
AC(8-OH)
AC(10-OH)
AC(10:0)
AC(9:0)
Dimethylglycine
Valine
Glycero
P-Ethanolamine
VIP Score
H
Glycolysis
TCA Cycle
Post/Pre Ratio
Glucose
Hexose-P
Fructose-bisP
Glyceraldehyde 3-P
bis-P-Glycerate
P-Glycerate
P-enolpyruvate
Pyruvate
Lactate
Citrate
α-Ketoglutarate
Succinate
Fumarate
Malate
I
Glycolysis
TCA Cycle
Post/Pre Ratio
J
Fatty Acids
Post/Pre Ratio
K
Fatty Acids
Post/Pre Ratio
L
Acylcarnitines
Post/Pre Ratio
Carnitine
M
Acylcarnitines
Post/Pre Ratio
Carnitine

◂**Fig. 1** Metabolic signatures of short/high-intensity and long/low-intensity training regimens. **A** During the training camp, whole blood from 28 Elite World Tour cyclists was sampled before and after a 1 h graded exercise test on an ergometer. **B** Whole blood lactate measurements (millimolar) as a function of normalized power output ($W \cdot kg^{-1}$) during the test. **C** During the same training camp, whole blood was sampled from 27 of the cyclists before and after a 180 km field test maintained in an aerobic regimen beneath the lactate threshold. Multivariate analyses including a principal component analysis (PCA) and a variable importance in projection (VIP) of partial least squares-discriminant analysis were performed on metabolomics data generated from the graded exercise test (**D**) and (**E**), or aerobic field test (**F**) and (**G**), respectively. Individual cyclist fold changes (post/pre) for metabolites involved in glycolysis and the tricarboxylic acid (TCA) cycle are shown as violin plots for the (**H**) graded exercise test and (**I**) aerobic field test. Individual cyclist fold changes (post/pre) for free fatty acids are shown as violin plots for the (**J**) graded exercise test and (**K**) aerobic field test. Individual cyclist fold changes (post/pre) for acylcarnitines are shown as violin plots for the (**L**) graded exercise test and (**M**) aerobic field test. *P* values (two-tailed paired *T*-test) for the post/pre-comparison are indicated as * < 0.05, ** < 0.01, *** < 0.001, and **** < 0.0001

(Fig. 2G, upper left). A pathway analysis of molecules in this cluster showed they were enriched in energy metabolism (TCA cycle), anabolism/oxidative stress response (pentose phosphate pathway [PPP], ascorbate metabolism, methionine and cysteine metabolism), amino acid metabolism (tyrosine, methionine, cysteine, alanine, aspartate), and protein glycosylation (sialic acid and amino sugar metabolism, N-glycan and keratan sulfate degradation). Metabolites contained in Cluster 2 opposed this trend, increasing primarily after the completion of Stages 4 and 6 (Fig. 2G, upper right). This cluster pertained to oxidative stress (ascorbate metabolism, glutathione metabolism) and energy metabolism (pyridoxine and pyruvate metabolism, glycolysis and gluconeogenesis). Meanwhile, Cluster 3 described molecules that are elevated after the completion of Stage 1 and progressively decrease throughout Stage 6 and are related primarily to fatty acid activation (Fig. 2G, lower left). Finally, molecules that decreased after the beginning of the race and did not predominantly recover through Stage 6 were described by Cluster 4 and enriched for the metabolism of amino acids, nucleotides, and nicotinamide (Fig. 2G, lower right).

3.3 Longitudinal Effects of Cycling on Energy Metabolism

Considering the enrichment of glycolysis, the PPP, and the TCA cycle from the systematic analysis of untargeted metabolomics, we then manually interrogated each of these pathways (Fig. 3A). Intermediates of the oxidative phase of the PPP including gluconolactone-6-phosphate and 6-phosphogluconate tend to increase after each stage (or significantly increase after Stage 6 or 4, respectively) (Fig. 3B). Meanwhile, non-oxidative intermediate sedoheptulose 7-phosphate decreased, while the pool of pentose phosphate isobars tended to increase after each stage (Fig. 3B). At steady state, these results suggest that the PPP is activated in response to cycling, which is supported by the progressive increase in glucose 6-phosphate throughout the race (Fig. 3C). Glucose phosphorylation by hexokinase commits it towards intracellular catabolism through both the PPP and glycolysis. Significantly increased glucose after Stage 1 indicates ongoing glycogenolysis to fuel these processes. Utilization of glycolysis is especially apparent in Stage 1 given the decrease in glycolytic intermediates and the increase in the end-products pyruvate and lactate (Fig. 3C). Interestingly, the accumulation of lactate after each successive stage is lower, suggesting either a routing of carbon into the mitochondria to fuel oxidative phosphorylation or a progressive loss in glycolytic capacity in these cyclists as fatigue accumulates. While citrate increases (significantly after Stage 6), additional TCA cycle intermediates succinate, fumarate, and malate accumulate after each stage, though to a lesser degree throughout the race (Fig. 3D). Meanwhile, the respective amino acid products of transamination reactions (alanine/pyruvate, aspartate/malate, glutamine/glutamate/α-ketoglutarate) inversely mirror their carboxylate counterparts, suggesting that these amino acids are consumed via transamination reactions to fuel the TCA cycle and maintain nitrogen homeostasis (Fig. 3E).

3.4 Longitudinal Effects of Cycling on Lipid Metabolism

In addition to the use of glucose and amino acid-derived carbon to fuel the TCA cycle, fat also serves as a fuel source especially under aerobic conditions of exercise. As such, we performed untargeted lipidomics to assess the relative levels of lipids throughout the race, which enabled relative quantification of 958 lipids after data curation (Table 1 of the ESM). Of all the lipid classes profiled, acylcarnitines (AC) were the only class to significantly change after each stage (Fig. 3F). Analysis of the relative levels of individual AC revealed marked accumulations of short- and medium-chain acylcarnitines (SCAC and MCAC) after Stage 6, and two cyclists finished this stage with high levels of long-chain acylcarnitines (LCAC) (Fig. 3G). The levels of fatty acids were even more distinctly elevated after Stage 6 in all cyclists, though this accumulation begins to appear after Stage 4 (Fig. 3G). The oxidation of fatty acids is in part dependent on the availability of carnitine, which significantly decreased throughout the course of the race. Meanwhile the levels of the coenzyme A (CoA) precursor, pantothenate, remained unchanged aside from a slight, though significant, increase after Stage 4 (Fig. 3H).

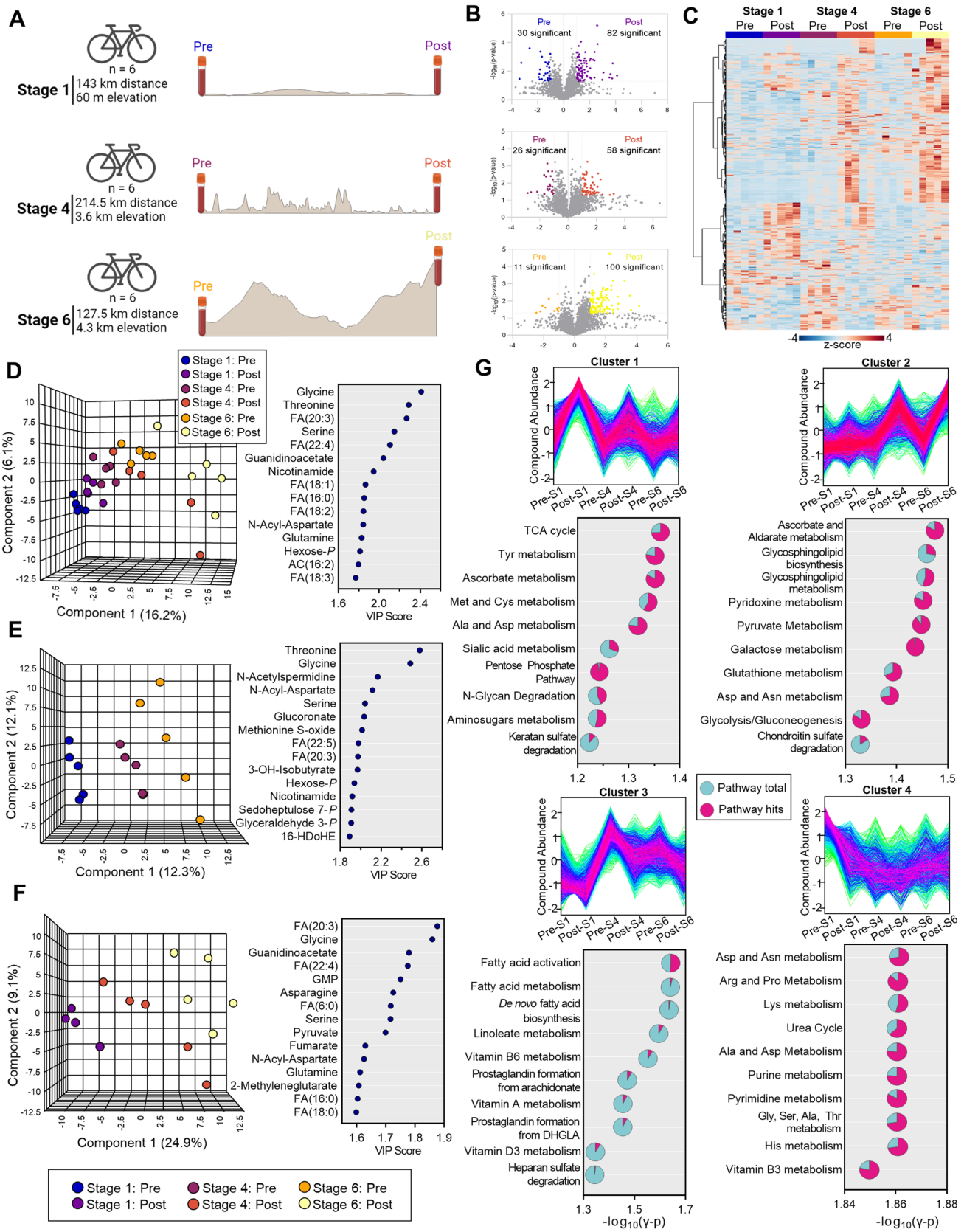
A
Stage 1
n = 6
143 km distance
60 m elevation
Pre
Post
Stage 4
n = 6
214.5 km distance
3.6 km elevation
Pre
Post
Stage 6
n = 6
127.5 km distance
4.3 km elevation
Pre
Post
B
Pre
30 significant
Post
82 significant
Pre
26 significant
Post
58 significant
Pre
11 significant
Post
100 significant
C
Stage 1
Stage 4
Stage 6
Pre
Post
z-score
D
Stage 1: Pre
Stage 1: Post
Stage 4: Pre
Stage 4: Post
Stage 6: Pre
Stage 6: Post
Component 1 (16.2%)
Component 2 (6.1%)
Glycine
Threonine
FA(20:3)
Serine
FA(22:4)
Guanidinoacetate
Nicotinamide
FA(18:1)
FA(16:0)
FA(18:2)
N-Acyl-Aspartate
Glutamine
Hexose-P
AC(16:2)
FA(18:3)
VIP Score
E
Component 1 (12.3%)
Component 2 (12.1%)
Threonine
Glycine
N-Acetylspermidine
N-Acyl-Aspartate
Serine
Glucoronate
Methionine S-oxide
FA(22:5)
FA(20:3)
3-OH-Isobutyrate
Hexose-P
Nicotinamide
Sedoheptulose 7-P
Glyceraldehyde 3-P
16-HDoHE
VIP Score
F
Component 1 (24.9%)
Component 2 (9.1%)
FA(20:3)
Glycine
Guanidinoacetate
FA(22:4)
GMP
Asparagine
FA(6:0)
Serine
Pyruvate
Fumarate
N-Acyl-Aspartate
Glutamine
2-Methyleneglutarate
FA(16:0)
FA(18:0)
VIP Score
Stage 1: Pre
Stage 1: Post
Stage 4: Pre
Stage 4: Post
Stage 6: Pre
Stage 6: Post
G
Cluster 1
Cluster 2
Cluster 3
Cluster 4
Compound Abundance
Pre-S1
Post-S1
Pre-S4
Post-S4
Pre-S6
Post-S6
TCA cycle
Tyr metabolism
Ascorbate metabolism
Met and Cys metabolism
Ala and Asp metabolism
Sialic acid metabolism
Pentose Phosphate Pathway
N-Glycan Degradation
Aminosugars metabolism
Keratan sulfate degradation
Ascorbate and Aldarate metabolism
Glycosphingolipid biosynthesis
Glycosphingolipid metabolism
Pyridoxine metabolism
Pyruvate Metabolism
Galactose metabolism
Glutathione metabolism
Asp and Asn metabolism
Glycolysis/Gluconeogenesis
Chondroitin sulfate degradation
Pathway total
Pathway hits
Fatty acid activation
Fatty acid metabolism
De novo fatty acid biosynthesis
Linoleate metabolism
Vitamin B6 metabolism
Prostaglandin formation from arachidonate
Vitamin A metabolism
Prostaglandin formation from DHGLA
Vitamin D3 metabolism
Heparan sulfate degradation
Asp and Asn metabolism
Arg and Pro Metabolism
Lys metabolism
Urea Cycle
Ala and Asp Metabolism
Purine metabolism
Pyrimidine metabolism
Gly, Ser, Ala, Thr metabolism
His metabolism
Vitamin B3 metabolism
-log10(γ-p)

◂**Fig. 2** Metabolomics of a multi-stage World Tour cycling race. **A** Whole-blood samples were isolated from cyclists before and after Stage 1, 4, and 6 of a consecutive seven-stage race and analyzed by mass spectrometry. **B** Volcano plots for Stage 1, 4, and 6 from top to bottom, respectively, with the number of significantly changed metabolites (fold change > 2, $p < 0.05$) indicated in the plot. **C** Hierarchical clustering analysis of features identified by metabolomics and lipidomics. **D** Partial least squares-discriminant analysis of identified metabolites and lipids before and after each stage (left) along with the top 15 compounds by variable importance in projection (right). Partial least squares-discriminant analysis of identified metabolites and lipids (**E**) before and (**F**) after each stage (left) along with the top 15 compounds by variable importance in projection (right). **G** Four distinct longitudinal signatures were determined by fuzzy c-means clustering. Compounds with patterns matching the top four clusters were analyzed to determine significantly enriched pathways in each cluster. Pathways for each cluster are organized by $-\log10(\gamma\ p$ value), with the number of pathway hits (pink) plotted as a fraction of pathway total (turquoise)

3.5 Individual Cyclist Metabolomics as a Function of Performance

The penultimate stage of the race consisted of a 127.5 km course through a mountainous region that finished with a first category climb (7% average grade) over the final 7.5 km (Fig. 4A). Cyclists 1 and 2 managed to outpace the other three throughout this stage, which was driven in part by the final vertical ascent (Fig. 4B). To identify metabolite signatures that associate with performance during this period of the race, we correlated average speed with metabolite levels in blood sampled immediately after Stage 6. Top correlates pertained predominantly to oxidation of fatty acids [AC(18:2), AC(18:1), AC(16:0), AC(18:0), AC(18:3), AC(3:1), FA(6:0), and pantothenate], nitrogen homeostasis (5-hydoxyisourate, 5-methylthioadenosine, 4-acetoamidobutanoate, lysine, spermidine, and spermine), and energy metabolism (glyceraldehyde 3-phopshate, succinate) (Fig. 4C, D). To expand analysis of personalized metabolic profiles across the entirety of the race, a sparse PLS-DA revealed a similar trend as the speed and output data, with the fastest cyclists 1 and 2 clustering together along the Component 2 axis (Fig. 4E). The top ten metabolites that contribute to the clustering pattern along this axis were enriched for intermediates of fatty acid oxidation (Fig. 4F). Indeed, Cyclists 1 and 2 maintained the highest levels of the CoA precursor pantothenate and LCAC throughout the duration of Stages 1, 4, and 6 (Fig. 4G). Cyclist 1, who was the top-performing cyclist in this cohort, had persistently high levels of carnitine and the lowest levels of MCAC and long-chain fatty acids (Fig. 4G, H), suggesting maintenance of mitochondrial capacity and fatty acid oxidation throughout the race. In support, this cyclist also finished Stage 6 with the lowest levels of glycolytic intermediates, lactate, and succinate (Fig. 4I, J), along with a larger pool of NAD(H) (Fig. 4K), indicating a lower fatigue status that could sustain a faster pace towards the end of the race. This same cyclist also displayed the highest levels of arginine and polyamines (spermine, Fig. 2A of the ESM), argininosuccinate, 5-methylthioadenosine (Fig. 1B of the ESM), and the second highest levels of citrulline, but the lowest levels of S-adenosyl-methionine, creatinine, and phosphocreatine (Fig. 2B of the ESM) across all other team members. Most notably, Cyclist 1 showed the highest levels of reduced and oxidized glutathione (total glutathione pools), and methionine (Fig. 2C of the ESM), suggestive of the highest antioxidant capacity throughout competition among all cyclists monitored in this study.

4 Discussion

We used mass spectrometry-based metabolomics to define whole-blood molecular profiles associated with sustained low- to medium-intensity cycling during a 180 km aerobic training ride in comparison with a GXT to volitional exhaustion. To facilitate field sampling, we circumvented the needs for traditional phlebotomy and maintaining frozen samples as is traditionally required for metabolomics analyses through the implementation of dried blood sampling using volumetric absorptive microsampling [20]. Because these samples were taken from the same elite professional cyclists during a 1-week training camp prior to the season, they enable a paired comparison of molecular profiles as a function of exertion and serve to define blood profiles of humans performing at optimal capacity. Metabolite profiles of the GXT demonstrated characteristic accumulations of circulating lactate, a biomarker of performance capacity that has been traditionally used to guide training exercise [19, 27]. In addition, we were also able to quantify the extent to which upstream glycolytic intermediates are modulated to sustain lactate production. The accumulation of lactate occurs at a power output when the rate of lactate production exceeds that of oxidation, termed the "lactate threshold," which is dependent upon the ability to oxidize lactate into pyruvate for subsequent metabolism in the mitochondria [10, 28]. Exercise intensity dictates demand for ATP and drives skeletal muscle metabolic responses. At high exercise intensities, glycolysis is the primary source of ATP, which is produced at a faster rate through the activity of glycolytic enzymes phosphoglycerate kinase and pyruvate kinase in comparison to mitochondrial electron transport chain-fueled ATP synthase. The latter route for ATP synthesis is dependent on mitochondrial capacity, which becomes limited at higher workloads. Under hypoxic conditions or at high bioenergetic demand, mitochondrial respiration becomes uncoupled leading to an accumulation of succinate, which is released into the extracellular environment [7, 29] as a function of intracellular proton accumulation [30]. In line

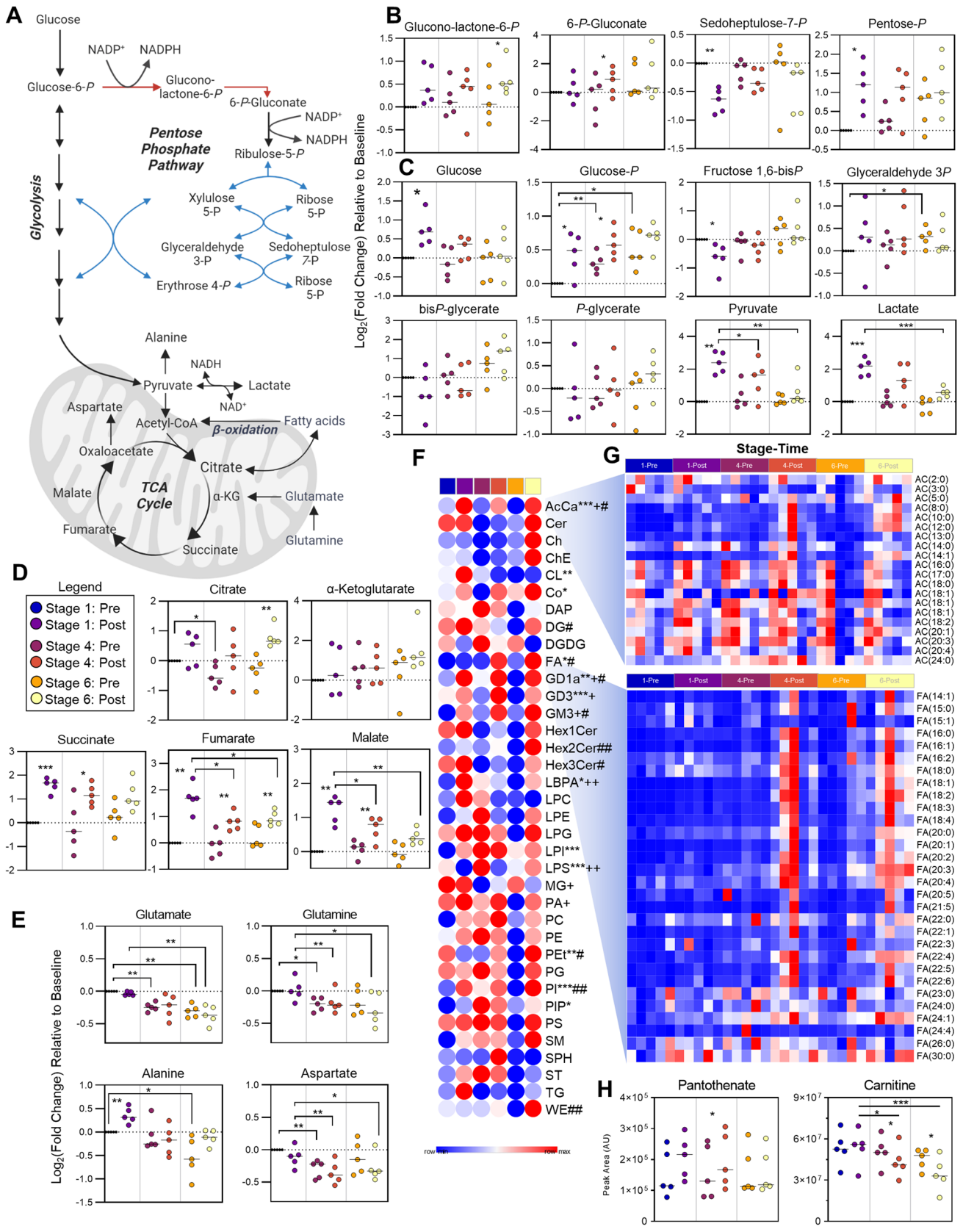
A
Glucose
NADP+
NADPH
Glucose-6-P
Glucono-lactone-6-P
6-P-Gluconate
NADP+
NADPH
Ribulose-5-P
Pentose Phosphate Pathway
Glycolysis
Xylulose 5-P
Ribose 5-P
Glyceraldehyde 3-P
Sedoheptulose 7-P
Erythrose 4-P
Ribose 5-P
Alanine
NADH
Pyruvate
Lactate
NAD+
Aspartate
Acetyl-CoA
β-oxidation
Fatty acids
Oxaloacetate
Citrate
Malate
TCA Cycle
α-KG
Glutamate
Fumarate
Succinate
Glutamine
B
Glucono-lactone-6-P
6-P-Gluconate
Sedoheptulose-7-P
Pentose-P
C
Glucose
Glucose-P
Fructose 1,6-bisP
Glyceraldehyde 3P
bisP-glycerate
P-glycerate
Pyruvate
Lactate
Log2(Fold Change) Relative to Baseline
D
Legend
Stage 1: Pre
Stage 1: Post
Stage 4: Pre
Stage 4: Post
Stage 6: Pre
Stage 6: Post
Citrate
α-Ketoglutarate
Succinate
Fumarate
Malate
E
Glutamate
Glutamine
Alanine
Aspartate
Log2(Fold Change) Relative to Baseline
F
AcCa***+#
Cer
Ch
ChE
CL**
Co*
DAP
DG#
DGDG
FA*#
GD1a**+#
GD3***+
GM3+#
Hex1Cer
Hex2Cer##
Hex3Cer#
LBPA*++
LPC
LPE
LPG
LPI***
LPS***++
MG+
PA+
PC
PE
PEt**#
PG
PI***##
PIP*
PS
SM
SPH
ST
TG
WE##
row min
row max
G
Stage-Time
1-Pre
1-Post
4-Pre
4-Post
6-Pre
6-Post
AC(2:0)
AC(3:0)
AC(5:0)
AC(8:0)
AC(10:0)
AC(12:0)
AC(13:0)
AC(14:0)
AC(14:1)
AC(16:0)
AC(17:0)
AC(18:0)
AC(18:1)
AC(18:1)
AC(18:1)
AC(18:2)
AC(20:1)
AC(20:3)
AC(20:4)
AC(24:0)
FA(14:1)
FA(15:0)
FA(15:1)
FA(16:0)
FA(16:1)
FA(16:2)
FA(18:0)
FA(18:1)
FA(18:2)
FA(18:3)
FA(18:4)
FA(20:0)
FA(20:1)
FA(20:2)
FA(20:3)
FA(20:4)
FA(20:5)
FA(21:5)
FA(22:0)
FA(22:1)
FA(22:3)
FA(22:4)
FA(22:5)
FA(22:6)
FA(23:0)
FA(24:0)
FA(24:1)
FA(24:4)
FA(26:0)
FA(30:0)
H
Pantothenate
Carnitine
Peak Area (AU)

◂**Fig. 3** Energy metabolism. **A** A pathway overview of energy metabolism is shown, along with stage comparisons of individual metabolite levels in **B** the pentose phosphate pathway (oxidative phase in red, non-oxidative phase in blue), **C** glycolysis, and the **D** tricarboxylic acid (TCA) cycle and the **E** amino acid transamination products. *P* values are depicted as * < 0.05, ** < 0.01, and *** < 0.001. **F** A heat map for group averages of the summed total for lipid classes is shown. **G** Relative levels at each stage/timepoint of acylcarnitines (top) and fatty acids (bottom) for each cyclist are shown. *P* values for Stage 1 Pre/Post comparison (* < 0.05, ** < 0.01, *** < 0.001), Stage 4 Pre/Post comparison (+) and Stage 6 Pre/Post comparison (#) are shown. **H** The peak areas at each stage/timepoint for coenzyme A precursor pantothenate and carnitine are shown

with previous findings [19], we observed increases of succinate that were comparable to that of lactate during the GXT. During the 180 km training session, however, when cyclists are functioning in aerobic conditions and primarily relying on fatty acid oxidation, succinate shows only modest increases while lactate remained unchanged.

High exercise intensities are predominantly sustained by carbohydrate oxidation, while low and medium intensities rely more upon catabolism of fatty acids for energy generation. Accordingly, we observed a substantially larger accumulation of long-chain fatty acids including the most abundant oleic and linoleic acid [31] after the 180 km aerobic training session in comparison with the GXT. The relatively higher levels of these fatty acids after the long training session indicate a longer period of fatty acid mobilization during this training test, which are subsequently converted intracellularly between acyl-CoA and acylcarnitine species for fatty acid oxidation within the mitochondria. The inability of mitochondria to continue oxidizing fatty acids, either owing to a lack of oxygen availability or the cessation of exercise, results in release of incompletely oxidized MCAC back into circulation. Short-chain acylcarnitines and MCAC notably accumulated significantly after the GXT in comparison to the lower intensity training session, indicating an abrupt shift in metabolism because of progressively increasing exercise intensity. The resulting accumulation of lactate exerts endocrine and autocrine actions by decreasing lipolysis [32] and mitochondrial fatty acid transport through decreased carnitine palmitoyltransferase I and II function [33]. Of note, MCAC are higher at baseline in patients with type 2 diabetes mellitus [34, 35], sepsis [36, 37], and post-acute sequelae of severe acute respiratory syndrome coronavirus 2 infection [38], and indicate that metabolomic signatures of acute exercise-induced fatigue resemble those of chronic diseases in which metabolic and mitochondrial dysfunction or impairment play an important pathogenic role.

When translated into a World Tour cycling competition, the metabolomic signatures presented herein enable the assessment of workload and performance. For instance, the most significantly enriched pathway in Cluster 1, which described compounds that accumulate the most after Stage 1, was the TCA cycle. This stage was characterized by long stretches of flat terrain with few hills that finished with a field sprint, which demanded higher workloads in line with the profiles seen in the GXT to volitional exhaustion. Notably, lactate and succinate both accumulated in circulation during this stage as well, thus indicating the high degree of exertion and fatigue in these cyclists after the sprint. In contrast, Stages 4 and 6 involved more climbing, and Stage 6 finished at the highest elevation of the race. Accordingly, we observed profiles indicating a predominant reliance on fat oxidation, as reflected by the accumulation of fatty acids and MCAC after the stage.

While this study only profiled the longitudinal patterns of five professional cyclists, the correlation of metabolic profiles with speed revealed interesting patterns. The slowest two cyclists during Stage 6 finished with the lowest levels of LCAC and the highest levels of circulating succinate, the latter of which was a marker of fatigue in the GXT. It is interesting to note that these two cyclists also had the highest levels of circulating glucose after Stage 1, as well as the highest lactate after Stages 1 and 4. This signature indicates that these two cyclists were more reliant on glycolysis early in the race, accessing stored glycogen to sustain output. As such, they may have depleted stores and began to fatigue more quickly than their teammates, thus resulting in poorer performance towards the end of the race. Meanwhile, the fastest two cyclists had lower succinate and higher LCAC after Stage 6, indicating ongoing aerobic fatty acid oxidation despite generating the highest power output and speed on the final ascent. Longitudinal characterization of all three sampled stages during the race revealed that these two cyclists maintained the highest levels of LCAC across this cohort, along with the highest level of CoA precursor pantothenate (vitamin B_5). Furthermore, Cyclist 1 had the lowest markers of incompletely oxidized fatty acids, along with the highest level of carnitine. This cyclist maintained the highest LT measured during training camp (Fig. 1B) and was the only individual who did not deviate from the metabolic trajectory in the World Tour identified by PLS-DA (Fig. 2D). This cyclist also had higher levels of branched-chain amino acids (BCAA) than the other cyclists, especially prominent after Stage 6 when isoleucine, leucine, and valine reached levels of 120, 219, and 264 μM, respectively (Fig. 3 of the ESM). In addition to its role in fatty acid oxidation, CoA plays a predominant role in BCAA catabolism, and its biosynthesis may be tied to the LT [19]. While plasma levels of BCAA have been reported to change in response to exercise duration and work load [39–41], BCAA oxidation propensity is also tied to endurance capacity [42]. These results indicate that high-performing elite cyclists have an increased capacity to maintain mitochondrial metabolism and oxidative phosphorylation at high workloads and

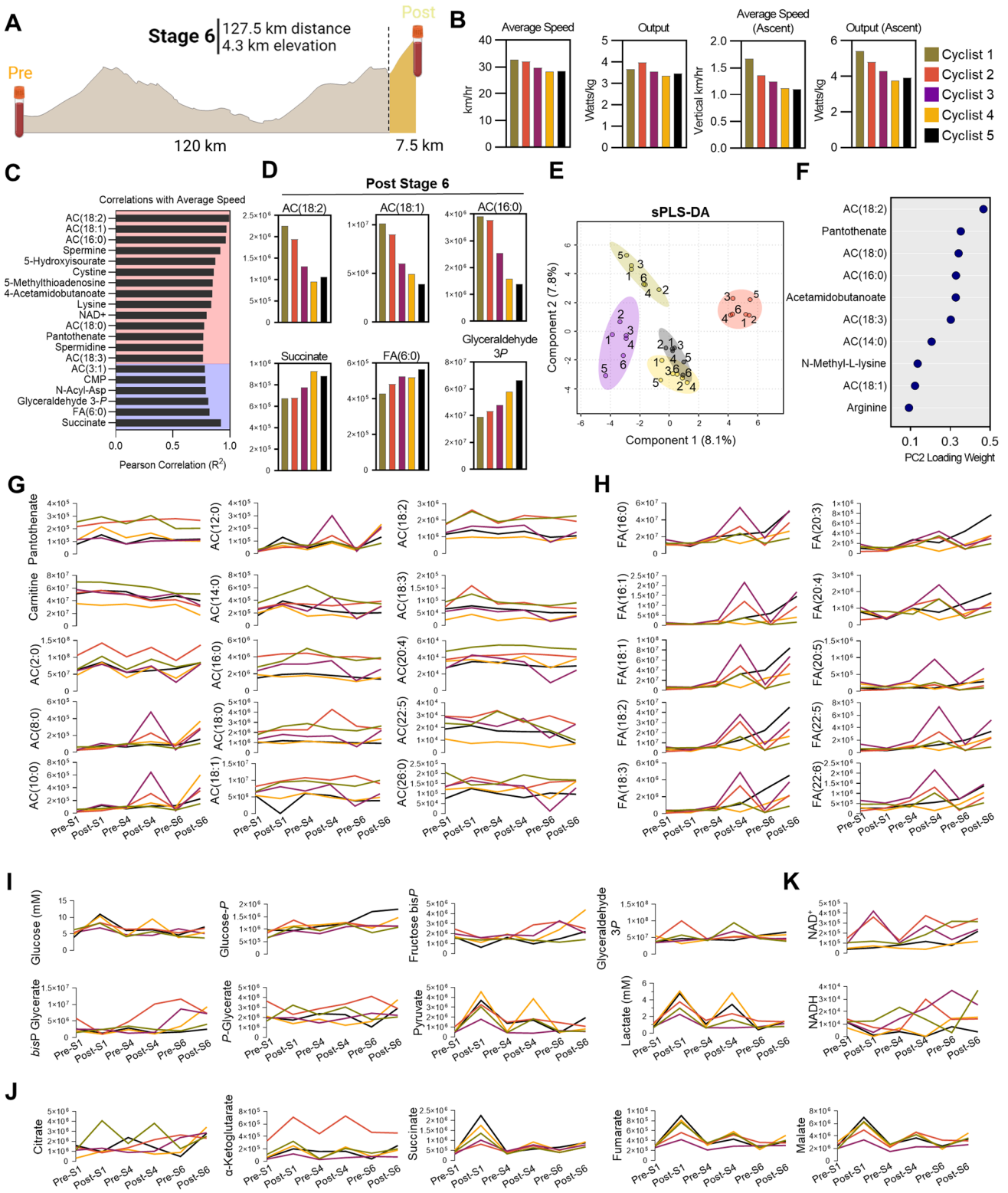

substantiate prior findings that cyclists' performance correlates with higher lactate clearance capacity at a comparable power output. [12]

Sports performance has both genetic and environmental influencing factors. Indeed, elite performance does have a basis in intensive training regimens. [43] While genetic

◂**Fig. 4** Individual cyclist analysis. **A** Metabolite, lipid, and training peaks functional cycling data for the entirety of Stage 6, along with training peaks during the final 7.5 km climb were analyzed. **B** Average speed and output for Stage 6, as well as the average speed and output of the final 7.5 km are plotted by individual cyclist. **C** Pearson correlation coefficients (R^2) for the top 20 Post-Stage 6 metabolite correlates with average speed during Stage 6 are shown, with positive correlates indicated in the red background and negative correlates indicated in the blue background. **D** Abundances (*y*-axis values are peak area top, given in arbitrary units) for each cyclist of the top three positive (top) and negative (bottom) correlates with average speed are shown. **E** A sparse partial least squares-discriminant analysis (sPLS-DA) is shown, with samples color coded according to cyclist and timepoint indicated as 1–6, where 1 = Stage 1-Pre consecutively up to 6 = Stage 6-Post. **F** The top ten loadings for principal component 2 are plotted. Longitudinal profiles during the course of the race for **G** acylcarnitines, **H** free fatty acids, **I** glycolysis, **J** tricarboxylic acid cycle, and **K** NAD + /NADH in each cyclist are shown as line graphs, with timepoints indicated on the bottom *x*-axis and abundance indicated on the *y*-axis as peak area (arbitrary units) except for glucose and lactate, for which the absolute concentrations are reported (millimolar)

factors are not as capable of distinguishing elite athletes on their own, a combination of Genome-Wide Association Studies (GWAS) with metabolomics using a metabolic quantitative trait loci analysis revealed significant associations between metabolite levels and genetic features [44]. One such metabolic quantitative trait loci is an association between the endocannabinoid linoleoyl ethanolamide and vascular non-inflammatory molecule 1 (VNN1), which functions as a pantetheinase, an enzyme that plays an integral role in the recycling of pantothenate to promote mitochondrial activity [45]. It is therefore interesting to consider the role that VNN1, or additional effectors of CoA/carnitine biosynthesis and fatty acid oxidation, may play in training, fatigue, and performance, especially in light of the putative association between this pathway and cyclist performance presented here. Ultimately, the complementarity of this approach holds future promise for the personalization of training regimens for sports performance and exercise prescription to treat metabolic syndrome [46] and improve cancer survivorship [47, 48]. The use of dried blood sampling enables these studies and allows for applicability to the general population.

5 Conclusions

The study shows that field sample collection for metabolomics analyses in professional elite athletes is feasible and informative of athlete condition and ultimate performance. The combination of lower cost high-throughput omics strategies and field sampling for remote collection without a phlebotomist can democratize omics technologies by making them accessible logistically and economically to all athletes, from recreational to elite athletes. Although limited by its observational nature, these studies provide a unique view into the metabolism of elite athletes performing at the best of their abilities both during training and in competition. Many of the cyclists profiled here are globally competitive and have stage and race wins to their names. As such, these profiles provide a view into bioenergetics and metabolic physiology of optimal human performance. The use of dried blood sampling enables these studies and allows for applicability to the general population. While the present study is limited to the integration of metabolomics and lipidomics profiling, future studies will involve the applications of orthogonal molecular characterization of samples from dried blood spots, such as proteomics.

Supplementary Information The online version contains supplementary material available at https://doi.org/10.1007/s40279-023-01846-9.

Declarations

Funding Research reported in this publication was funded by the National Institute of General and Medical Sciences (RM1GM131968 to ADA), and R01HL146442 (ADA), R01HL149714 (ADA), R01HL148151 (ADA), R01HL161004 (ADA), and R21HL150032 (ADA) from the National Heart, Lung, and Blood Institute. The content is solely the responsibility of the authors and does not necessarily represent the official views of the National Institutes of Health.

Conflict of interest Travis Nemkov, Kirk C. Hansen, and Angelo D'Alessandro are co-founders of Omix Technologies, Inc. Travis Nemkov, Angelo D'Alessandro, and Iñigo San-Millán are co-founders of Altis Biosciences. Angelo D'Alessandro is a SAB member or consultant for Hemanext Inc, Macopharma, and Forma Therapeutics Inc. Francesca Cendali, Davide Stefanoni, Janel L. Martinez have no conflicts of interests that are directly relevant to the content of this article.

Ethics approval All study procedures were conducted in accordance with the Declaration of Helsinki and in accordance with a predefined protocol that was approved by the Colorado Multiple Institutional Review Board (COMIRB 17-1281).

Consent to participate Written informed consent was obtained from all subjects.

Consent for publication While identifying information is intentionally omitted from this article to maintain anonymity, all subjects provided written informed consent for publication.

Availability of data and material All data generated as part of this study are presented in the supplementary materials.

Code availability No code was generated as part of this study.

Author contributions ISM, TN, and AD designed the studies. JLM and ISM performed exercise tests and collected the samples in laboratory and field settings. TN, FC, DS, KCH, and AD performed omics analyses. TN performed data analyses and prepared figures. TN wrote the first version of the manuscript, which was finalized with AD and reviewed and approved by all co-authors.

References

1. Moghetti P, Bacchi E, Brangani C, Donà S, Negri C. Metabolic effects of exercise. Front Horm Res. 2016;47:44–57.
2. Contrepois K, Wu S, Moneghetti KJ, Hornburg D, Ahadi S, Tsai M-S, et al. Molecular choreography of acute exercise. Cell. 2020;181:1112-30.e16.
3. Pontzer H, Yamada Y, Sagayama H, Ainslie PN, Andersen LF, Anderson LJ, et al. Daily energy expenditure through the human life course. Science. 2021;373:808–12.
4. Costantino S, Paneni F, Cosentino F. Ageing, metabolism and cardiovascular disease: mechanisms of cardiovascular ageing. J Physiol. 2016;594:2061–73.
5. Ruiz-Canela M, Hruby A, Clish CB, Liang L, Martínez-González MA, Hu FB. Comprehensive metabolomic profiling and incident cardiovascular disease: a systematic review. J Am Heart Assoc. 2017;6: e005705.
6. Hanahan D. Hallmarks of cancer: new dimensions. Cancer Discov. 2022;12:31–46.
7. Chouchani ET, Pell VR, Gaude E, Aksentijević D, Sundier SY, Robb EL, et al. Ischaemic accumulation of succinate controls reperfusion injury through mitochondrial ROS. Nature. 2014;515:431–5.
8. O'Neill LAJ, Kishton RJ, Rathmell J. A guide to immunometabolism for immunologists. Nat Rev Immunol. 2016;16:553–65.
9. Traxler L, Herdy JR, Stefanoni D, Eichhorner S, Pelucchi S, Szücs A, et al. Warburg-like metabolic transformation underlies neuronal degeneration in sporadic Alzheimer's disease. Cell Metab. 2022;34:1248-63.e6.
10. Brooks GA. The science and translation of lactate shuttle theory. Cell Metab. 2018;27:757–85.
11. Poole DC, Rossiter HB, Brooks GA, Gladden LB. The anaerobic threshold: 50+ years of controversy. J Physiol. 2021;599:737–67.
12. San-Millán I, Brooks GA. Assessment of metabolic flexibility by means of measuring blood lactate, fat, and carbohydrate oxidation responses to exercise in professional endurance athletes and less-fit individuals. Sports Med. 2018;48:467–79.
13. Sakaguchi CA, Nieman DC, Signini EF, Abreu RM, Catai AM. Metabolomics-based studies assessing exercise-induced alterations of the human metabolome: a systematic review. Metabolites. 2019;9:164.
14. Khoramipour K, Sandbakk Ø, Keshteli AH, Gaeini AA, Wishart DS, Chamari K. Metabolomics in exercise and sports: a systematic review. Sports Med. 2022;52:547–83.
15. Morville T, Sahl RE, Moritz T, Helge JW, Clemmensen C. Plasma metabolome profiling of resistance exercise and endurance exercise in humans. Cell Rep. 2020;33: 108554.
16. Schranner D, Schönfelder M, Römisch-Margl W, Scherr J, Schlegel J, Zelger O, et al. Physiological extremes of the human blood metabolome: a metabolomics analysis of highly glycolytic, oxidative, and anabolic athletes. Physiol Rep. 2021;9: e14885.
17. Al-Khelaifi F, Diboun I, Donati F, Botrè F, Alsayrafi M, Georgakopoulos C, et al. A pilot study comparing the metabolic profiles of elite-level athletes from different sporting disciplines. Sports Med Open. 2018;4:2.
18. Nemkov T, Skinner SC, Nader E, Stefanoni D, Robert M, Cendali F, et al. Acute cycling exercise induces changes in red blood cell deformability and membrane lipid remodeling. Int J Mol Sci. 2021;22:E896.
19. San-Millán I, Stefanoni D, Martinez JL, Hansen KC, D'Alessandro A, Nemkov T. Metabolomics of endurance capacity in World Tour professional cyclists. Front Physiol. 2020;11:578.
20. Volani C, Caprioli G, Calderisi G, Sigurdsson BB, Rainer J, Gentilini I, et al. Pre-analytic evaluation of volumetric absorptive microsampling and integration in a mass spectrometry-based metabolomics workflow. Anal Bioanal Chem. 2017;409:6263–76.
21. Cendali F, D'Alessandro A, Nemkov T. Dried blood spot characterization of sex-based metabolic responses to acute running exercise. Anal Sci Adv. 2023;4:37–48.
22. Catala A, Culp-Hill R, Nemkov T, D'Alessandro A. Quantitative metabolomics comparison of traditional blood draws and TAP capillary blood collection. Metabolomics. 2018;14:100.
23. Nemkov T, Hansen KC, D'Alessandro A. A three-minute method for high-throughput quantitative metabolomics and quantitative tracing experiments of central carbon and nitrogen pathways. Rapid Commun Mass Spectrom. 2017;31:663–73.
24. Reisz JA, Zheng C, D'Alessandro A, Nemkov T. Untargeted and semi-targeted lipid analysis of biological samples using mass spectrometry-based metabolomics. Methods Mol Biol. 2019;1978:121–35.
25. Melamud E, Vastag L, Rabinowitz JD. Metabolomic analysis and visualization engine for LC-MS data. Anal Chem. 2010;82:9818–26.
26. Chong J, Soufan O, Li C, Caraus I, Li S, Bourque G, et al. MetaboAnalyst 4.0: towards more transparent and integrative metabolomics analysis. Nucleic Acids Res. 2018;46:W486–94.
27. San-Millán I, González-Haro C, Sagasti M. Physiological differences between road cyclists of different categories: a new approach. 733. Med Sci Sports Exerc. 2009;41:64–5.
28. Brooks GA. Anaerobic threshold: review of the concept and directions for future research. Med Sci Sports Exerc. 1985;17:22–34.
29. D'Alessandro A, Moore HB, Moore EE, Reisz JA, Matthew J, Ghasabyan A, et al. Plasma succinate is a predictor of mortality in critically injured patients. J Trauma Acute Care Surg. 2017.
30. Reddy A, Bozi LHM, Yaghi OK, Mills EL, Xiao H, Nicholson HE, et al. pH-gated succinate secretion regulates muscle remodeling in response to exercise. Cell. 2020;183:62-75.e17.
31. Buchanan CDC, Lust CAC, Burns JL, Hillyer LM, Martin SA, Wittert GA, et al. Analysis of major fatty acids from matched plasma and serum samples reveals highly comparable absolute and relative levels. Prostaglandins Leukot Essent Fatty Acids. 2021;168: 102268.
32. Liu C, Wu J, Zhu J, Kuei C, Yu J, Shelton J, et al. Lactate inhibits lipolysis in fat cells through activation of an orphan G-protein-coupled receptor, GPR81. J Biol Chem. 2009;284:2811–22.
33. San-Millan I, Sparagna GC, Chapman HL, Warkins VL, Chatfield KC, Shuff SR, et al. Chronic lactate exposure decreases mitochondrial function by inhibition of fatty acid uptake and cardiolipin alterations in neonatal rat cardiomyocytes. Front Nutr. 2022;9: 809485.
34. Makrecka-Kuka M, Sevostjanovs E, Vilks K, Volska K, Antone U, Kuka J, et al. Plasma acylcarnitine concentrations reflect the acylcarnitine profile in cardiac tissues. Sci Rep. 2017;7:17528.
35. Sun L, Liang L, Gao X, Zhang H, Yao P, Hu Y, et al. Early prediction of developing type 2 diabetes by plasma acylcarnitines: a population-based study. Diabetes Care. 2016;39:1563–70.
36. Langley RJ, Tsalik EL, van Velkinburgh JC, Glickman SW, Rice BJ, Wang C, et al. An integrated clinico-metabolomic model improves prediction of death in sepsis. Sci Transl Med. 2013;5:195ra95.
37. Rogers AJ, McGeachie M, Baron RM, Gazourian L, Haspel JA, Nakahira K, et al. Metabolomic derangements are associated with mortality in critically ill adult patients. PLoS ONE. 2014;9: e87538.
38. Guntur VP, Nemkov T, de Boer E, Mohning MP, Baraghoshi D, Cendali FI, et al. Signatures of mitochondrial dysfunction and impaired fatty acid metabolism in plasma of patients with post-acute sequelae of COVID-19 (PASC). Metabolites. 2022;12:1026.

39. Poortmans JR, Siest G, Galteau MM, Houot O. Distribution of plasma amino acids in humans during submaximal prolonged exercise. Eur J Appl Physiol. 1974;32:143–7.
40. Refsum HE, Gjessing LR, Strømme SB. Changes in plasma amino acid distribution and urine amino acids excretion during prolonged heavy exercise. Scand J Clin Lab Invest. 1979;39:407–13.
41. Ahlborg G, Felig P, Hagenfeldt L, Hendler R, Wahren J. Substrate turnover during prolonged exercise in man: splanchnic and leg metabolism of glucose, free fatty acids, and amino acids. J Clin Invest. 1974;53:1080–90.
42. Overmyer KA, Evans CR, Qi NR, Minogue CE, Carson JJ, Chermside-Scabbo CJ, et al. Maximal oxidative capacity during exercise is associated with skeletal muscle fuel selection and dynamic changes in mitochondrial protein acetylation. Cell Metab. 2015;21:468–78.
43. Tucker R, Collins M. What makes champions? A review of the relative contribution of genes and training to sporting success. Br J Sports Med. 2012;46:555–61.
44. Al-Khelaifi F, Diboun I, Donati F, Botrè F, Abraham D, Hingorani A, et al. Metabolic GWAS of elite athletes reveals novel genetically-influenced metabolites associated with athletic performance. Sci Rep. 2019;9:19889.
45. Giessner C, Millet V, Mostert KJ, Gensollen T, Vu Manh T-P, Garibal M, et al. Vnn1 pantetheinase limits the Warburg effect and sarcoma growth by rescuing mitochondrial activity. Life Sci Alliance. 2018;1: e201800073.
46. Grundy SM, Cleeman JI, Daniels SR, Donato KA, Eckel RH, Franklin BA, et al. Diagnosis and management of the metabolic syndrome: an American Heart Association/National Heart, Lung, and Blood Institute Scientific Statement. Circulation. 2005;112:2735–52.
47. Hojman P, Gehl J, Christensen JF, Pedersen BK. Molecular mechanisms linking exercise to cancer prevention and treatment. Cell Metab. 2018;27:10–21.
48. Marker RJ. Cancer related fatigue mediates the relationships between physical fitness and attendance and quality of life after participation in a clinical exercise program for survivors of cancer. Qual Life Res. 2022;31(11):3201–10.